BIOLOGICAL SCIENCES - Plant Biology

Probing the electric field across thylakoid membranes in cyanobacteria

Stefania Viola[a,b], Benjamin Bailleul[a], Jianfeng Yu[b], Peter Nixon[b], Julien Sellés[a], Pierre Joliot[a], Francis-André Wollman[a,1]

[a]Laboratoire de Physiologie Membranaire et Moléculaire du Chloroplaste-UMR7141, IBPC, CNRS-Sorbonne Université, Paris, France.
[b]Department of Life Sciences, Imperial College – South Kensington Campus, London, UK.

[1]Corresponding author: Francis-André Wollman
Address: UMR7141 - IBPC, 13 rue Pierre et Marie Curie, 75005 Paris, France
Tel: +33 (0)1 58 41 50 12
Email: wollman@ibpc.fr

Keywords: Cyanobacteria, Photosynthesis, ElectroChromic Shift, Electron fluxes

Author contributions: S.V., B.B., J.S., P.J. and F.A.W. designed the experiments; S.V., B.B., J.S. and P.J. performed the experiments; S.V., B.B., J.S., and P.J. analysed the data; S.V., B.B., J.S., P.J. and F.A.W. wrote the manuscript, J.Y. and P.N. designed and generated the PSII- mutant.
The authors declare no conflict of interest.

Abstract

In plants, algae and some photosynthetic bacteria, the ElectroChromic Shift (ECS) of photosynthetic pigments, which senses the electric field across photosynthetic membranes, is widely used to quantify the activity of the photosynthetic chain. In cyanobacteria, ECS signals have never been used for physiological studies, although they can provide a unique tool to study the architecture and function of the respiratory and photosynthetic electron transfer chains, entangled in the thylakoid membranes. Here, we identified *bona fide* ECS signals, likely corresponding to carotenoid band shifts, in the model cyanobacteria *Synechococcus elongatus* PCC7942 and *Synechocystis sp.* PCC6803. These band shifts, most likely originating from pigment(s) located in photosystem I, have highly similar spectra in the two species and can be best measured as the difference between the absorption changes at 500-505 nm and the ones at 480-485 nm. These signals respond linearly to the electric field and display the basic kinetic features of ECS as characterized in other organisms. We demonstrate that these probes are an ideal tool to study photosynthetic physiology *in vivo*, e.g. the fraction of PSI centres that are pre-bound by plastocyanin/cytochrome c_6 in darkness (about 60% in both cyanobacteria, in our experiments), the conductivity of the thylakoid membrane (largely reflecting the activity of the ATP synthase) or the steady-state rates of the photosynthetic electron transport pathways.

Significance statement

Cyanobacteria were the first organisms to develop oxygenic photosynthesis using water as a source of electrons. Today they remain widespread primary photosynthetic producers and they hold a high biotechnological potential. In cyanobacteria, respiration and photosynthesis are interconnected in a complex network of electron fluxes. The study of cyanobacterial physiology is hampered by the lack of techniques allowing a direct measurement of the transmembrane electric field which develops across their photosynthetic/respiratory membranes. Here, we characterized a probe of the transmembrane electric field, based on the ElectroChromic Shifts of carotenoids, thus opening unprecedented avenues to bioenergetics studies of these major photosynthetic organisms.

\body

Introduction

About 2,8 billion years ago started the great oxygenation event caused by cyanobacteria, the first organisms to perform oxygenic photosynthesis using two photosystems linked in series and water as an electron donor (1, 2). In cyanobacteria, the photosynthetic and the respiratory electron transfer chains are both located in the thylakoid membranes and they share several redox components (3), giving rise to a complex network of electron fluxes. Moreover, cyanobacteria are proposed to house two pathways for a photosystem II (PSII)-independent electron flow towards photosystem I (PSI). One is mediated by the NADPH:plastoquinone oxidoreductase (NDH) complexes (4, 5), the other being an NDH-independent but ferredoxin-dependent pathway. The molecular nature of the latter requires further elucidation, following the characterization of a mutant showing some altered electron flow (6). No accurate estimation of the physiological turnover rates of these pathways is available so far.

The study of cyanobacterial photosynthetic fluxes is further complicated by the fact that current methods like PSII fluorescence (7) and PSI absorption spectroscopy (8) measure distinct variables that cannot be quantitatively compared without potential biases. Moreover, the quantitative interpretation of fluorescence parameters in cyanobacteria is hampered by a number of pitfalls (9, 10). A powerful tool to measure photosynthetic activity, extensively used in plants, algae and several photosynthetic bacteria, is the ElectroChromic Shift (ECS) of photosynthetic pigments (11, 12), which is based on a physical phenomenon known as the Stark effect. This method relies on the shift of the absorption spectrum of some photosynthetic pigments in the thylakoid membrane in response to changes in the trans-membrane electric field generated by the photosynthetic activity. Upon illumination, each of the components of the photosynthetic chain participates in either the formation (PSII, cytochrome b_6f, PSI) or the dissipation (ATP synthase) of a proton motive force, which has an electric and an osmotic component. Light-induced ECS signals can thus be used to assess the activities and/or relative amounts of each of the photosynthetic complexes (13). ECS measurements can also be used to calculate the turnover rates of the photosystems during illumination (14, 15) and to determine the levels of the pre-existing electrochemical proton gradient in the dark (16, 17).

In chlorophytes, the electrochromic signals in the 450-600 nm region of the spectrum are attributed to a combination of carotenoid and chlorophyll *b* band shifts (12, 18). ECS signals corresponding, in the same spectral region, only to carotenoid band shifts have been described

in red and brown algae (19), as well as in microalgae (20) and photosynthetic bacteria (21). In the case of cyanobacteria, earlier studies concluded to the absence of light-induced signals that could be ascribed to carotenoid band shifts (19, 20), in contrast with subsequent reports of putative ECS signals in intact cells (22, 23) and isolated PSI complexes (24) from different species. Still no ECS-based measurements have ever been used for physiological studies.

Here, we identified *bona fide* ECS signals in the model cyanobacteria *Synechococcus elongatus* PCC7942 and *Synechocystis sp.* PCC6803. We show that these signals are consistent with carotenoid band shifts, do not originate from PSII, are linearly proportional to the light-induced transmembrane electric field and display all the kinetic properties of ECS. We provide conclusive evidence for a rapid phase in the kinetics of re-reduction of P_{700}, the special pair of PSI, *in vivo* in both cyanobacteria. We also demonstrate that the identified electrochromic probes can be used to study the changes in membrane permeability and the electron flow rates.

Results and Discussion

Flash-induced carotenoid band shifts in S. elongatus and Synechocystis

We recorded the spectra of the absorption changes induced by single-turnover saturating flashes in *S. elongatus*. Cells were placed in anaerobic conditions in presence of the PSII inhibitors DCMU and hydroxylamine (HA), to eliminate the absorption changes produced by PSII turnovers. We recorded these spectra 19 ms after the flash, followed by five detecting flashes given 100 ms apart, to minimize the contribution of redox-dependent absorption changes that mostly relax before 19 ms (Fig. S2). As shown in Fig. 1A, the decay of the absorption changes was uniform in the 450-550 nm region: all spectra show two minima peaking around 455 and 485 nm, three maxima at 450, 470 and 500 nm and a broad featureless positive region between 510 and 540 nm. On the edges of the recorded spectral region was a transient bleaching at 420-425 nm and 554 nm that we attribute to the oxidation of the c-type haem of cytochrome *f* (and possibly of cyt c_6), and an absorbance increase at 435 nm and 560 nm, that we attribute to the reduction of the b_H haem of cyt *b* (25). After 100 ms, the homothetic decay in the 450-550 nm region is consistent with only one signal contributing to the long-lived absorption changes that we attribute to ECS. Indeed, after normalization on the (500 - 485 nm) difference (Fig. S3A), the spectra recorded at the different times were superimposed in the 450-550 nm region, except for a small bleaching at 510-520 nm in the 19 ms recording. The identified ECS spectrum is very similar to the carotenoid band shifts

described in red and brown algae and in photosynthetic bacteria (19–21), with peaks located at 30 nm intervals. To further remove the spectral contribution of cytochrome redox changes we used the redox catalyst PMS, which induces an artificial cyclic flow around PSI that bypasses the cytochrome b_6f complex (26). Indeed, in its semi-reduced form, PMS is both an electron acceptor and donor and once fully reduced by PSI, it partitions into the lumen and donates electrons to PSI, probably through plastocyanin (27), releasing protons. The spectra of flash-induced absorption changes were recorded in presence of 15 µM PMS in DCMU- and HA-treated *S. elongatus* cells. Addition of PMS eliminated most of the contribution from the b haems and from c-type cytochromes. Only a minor contribution of those signals remained 5 ms after the flash, which can be visualized in the 420-440 nm region, and it relaxed completely within 100 ms (Fig 1B and S3B). We therefore consider that the spectra measured after 100 ms are pure ECS spectra which present minima at 430, 455, 485 nm and 560 nm, maxima at 450, 470 and 500 nm and a broad positive region at 510-540 nm. We also note that the addition of PMS caused a progressive decrease in the ECS amplitude in the green region of the spectrum (510 to 540 nm) in *S. elongatus*. This is caused by the appearance of a negative signal peaking around 515 nm that superimposed itself to ECS during the time course of the experiment (about two hours between the forth and the back recordings, in anaerobic conditions). As shown in Fig. S4A and B and further discussed in the SI Appendix, the progressive bleaching was present also when recording spectra in absence of PMS, although to a much lesser extent. We do not have a direct evidence of the nature of such a signal, although the spectrum of the difference between the forth and the back recordings may also be due to a change in the band shift of a carotenoid. These spectral changes did not affect the amplitudes of the negative peak at 480-485 nm and the positive peak at 500-505 nm.

We investigated the presence of ECS in another commonly used cyanobacterium, *Synechocystis sp.* PCC6803. Fig. 1C and S3C show the spectra of flash-induced absorption changes recorded in presence of 15 µM PMS in DCMU and HA-treated cells. The spectra showed a predominant component with homothetic decay and a shape highly similar to the electrochromic signal of *S. elongatus*, except for a red shift of about 10 nm of the broad positive feature in the 510 - 540 nm region. Most notably, the difference between 480-485 nm and 500-505 nm was conserved. Again, the contribution of cyt *f* and cyt *b* redox signals was small in the presence of PMS, with the further addition of a non-homothetic negative signal present at 410 - 470 nm in the 5 ms recording. In the case of *Synechocystis*, minor spectral changes also appeared between the forth and the back recordings (Fig. S4C) but, again, they did not affect the 480-505 nm region.

The ECS gives a direct measure of the transmembrane electric field irrespectively of the molecular nature of the electrochromic pigments and of their location in the membrane. Even so, in *S. elongatus* and *Synechocystis* the ECS spectra suggest that such pigments are carotenoids. To also investigate their location, we recorded the ECS spectrum in a *Synechocystis* mutant lacking photosystem II (PSII, characterization in Fig. S5) and compared the long-lived absorption difference signals, when the redox spectral contributions have completely relaxed (i.e. >100 ms), with those in the wild type. The two strains presented remarkably similar spectra in the 470-510 nm region, both featuring the carotenoid shift we described so far (Fig. 2A). We noted spectral differences in the mutant in the blue and red sides of the spectrum (discussed in the SI Appendix, Fig. S6). We also looked whether phycobilisomes, although located at the thylakoid membrane surface, could contribute to the ECS signal. We measured the spectra of the absorption changes in the PAL mutant (Fig. 2B), lacking phycobilisomes (28, 29). The ECS signal proved much shorter-lived in this strain, which did not allow the extraction of a pure ECS spectrum (note the important redox contributions at 425-430 nm and 555-560 nm). Nevertheless, 5 ms after a flash, the spectra were similar in the mutant and wild type in the 480-510 nm region. Taken together, these results are consistent with the ECS signal originating from carotenoids located within PSI cores (see also SI Results and Discussion). It should be noted that variations in the absolute amplitude of ECS signals due to variations in the content of the pigment protein complex(es) harbouring the probes (e.g. PSI), will not affect the measurements, provided that ECS signals are proportional to the electric field (see below) and normalized to the ECS signal generated by a single-turnover saturating flash, which corresponds to one charge separation per active photosystem.

Examination of the above spectra shows that the ECS can be best measured by the difference between the absorption changes at 500-505 nm and at 480-485 nm in the two cyanobacteria: this difference is the one with the largest amplitude, which corrects for the absorption changes associated with the oxidation/reduction of P_{700}, c-type cytochromes and b haems (25, 30) and is not affected by the distortion observed in the green region of the spectrum. To further substantiate the attribution of the long-lived absorption difference to an ECS signal of appropriate lifetime and characteristic spectrum, we examined the kinetic prediction of this attribution. Indeed, the kinetics of an ECS signal after a single turnover flash display unique characteristics, being comprised of three phases: i- a fast rise ("*a* phase", completed in <100 μs) corresponding to photochemistry in PSII and PSI, ii- a second rise ("*b* phase", completed in ~10 ms) which corresponds to the electron transfer from PSII acceptors to PSI donors,

catalysed by the cytochrome b_6f, and iii- a phase of ECS decay ("*c* phase") reflecting the electric permeability of the thylakoid membrane (mostly the proton efflux catalysed by the ATP synthase).

Flash-induced ECS kinetics: the a phase and its use for monitoring the activity of photosystems

To test whether the fast rise in ECS that follows a single turnover flash corresponds to the contribution of active photosystems, we measured the PSI open centres (in conditions of PSII inhibition, adding HA and DCMU) using two independent methods. After a first saturating flash, generating a transmembrane electric field, a second one is applied at increasing time intervals and generates an additional electric field. The latter should be proportional to the fraction of P_{700} that has been re-reduced between the two flashes, which we measured in parallel by the absorption difference signals at 435 nm (Fig. 3). As described above, we performed these measurements in presence of PMS (*SI* Results and Discussion and Fig. S7) to remove cyt b_6f-related absorption changes at 435 nm and prevent back reactions within PSI. At 5 ms after the first flash, almost all P_{700} was reduced (see spectra in Fig. S3B and C) and the ECS increase upon a second flash was almost equal to the first one (Fig. 3A and B) indicating that only a small fraction (≤10%) of PSI remained closed after 5 ms. This fraction likely corresponds to PSI centres that are not connected to secondary donors and thus remain oxidized 5 ms after the actinic flash. Using this value at 5 ms to normalize the amount of PSI open centres (see Material and Methods), the kinetics measured with the ECS and the P_{700}^{+} absorption methods were superimposed (Fig. 3D), demonstrating that the *a* phase of the ECS signal gives a direct measurement of the fraction of open centres. It also indicates that this ECS signal shows a linear response to the variation of the transmembrane electric field, as it does in plants and green algae (11). The PSI reduction kinetics showed, in both cyanobacteria, two phases completed in ~100 µs and in ~3 ms, respectively (representative traces shown in Fig. 3C). The fast phase, having a half time of ~7 µs, suggests the presence *in vivo* in the dark of a fraction of PSI complexes (about 60% of the total) bound to reduced plastocyanin or cyt c_6. The half time for the electron transfer between the bound electron donor and P_{700} is close to that measured in plant chloroplasts (~ 4 µs) (31). The slower phase can be attributed to the diffusion time of plastocyanin or cyt c_6 molecules responsible for the reduction of the remaining fraction of PSI complexes; its half time (~200 µs) is also close to what was measured in chloroplast for the reaction between free plastocyanin and P_{700} (31–33). The fast PSI reduction phase was present also in absence of PMS (Fig. S8), indicating that it is not due

to a direct donation of electrons from PMS to PSI. Thus, a fast donation of electrons from a pre-bound electron donor to P_{700} does occur *in vivo* in both *S. elongatus* and *Synechocystis*.

The *a* phase, representing charge separations from active photosystems, can also be used to assess the PSI/PSII ratio. Fig. 4A shows representative traces of the flash-induced ECS kinetics in *S. elongatus* in the control or when PSII is inhibited by the addition of DCMU and HA. In the latter case, the *a* phase is solely due to PSI photochemistry and the comparison with the control allowed us to determine a PSI/PSII ratio of 2.3±0.5 (5 biological replicates) in *S. elongatus*, in line with previous reports, e.g. (34). The same experiment performed in *Synechocystis* (Fig S9C) also confirms the excess of PSI over PSII reaction centres.

Flash-induced ECS kinetics: b phase and decay

As mentioned above, a flash-induced ECS kinetics should display, after the fast rise ("*a* phase"), a second rise called "*b* phase" followed by a decay ("*c* phase") reflecting the dissipation of the transmembrane electric field. We note that in *S. elongatus* PSII inhibition caused an overall slowing down of the ECS decay (Fig 4A), allowing the observation of the slow electrogenic phase (maximal at 20 ms), due to the turnover of cyt b_6f (13). This "*b* phase" was, as expected for a proper ECS signal, a *bona fide* probe of electron transfer though the cytochrome b_6f since it was sensitive to PMS (Fig. S7A), which bypasses this complex, and to the quinone analogue DBMIB, which inhibits its turnover (Fig. S9A). The flash-induced ECS kinetics in *Synechocystis* had an overall faster decay than those in *S. elongatus*, preventing the observation of the *b* phase (Fig. S9B and C).

Since the ECS decay depends on the permeability of the thylakoid membrane, it reflects mostly the dissipation of the proton gradient by the ATP synthase. Counter-ion movements do also participate in modifying the membrane permeability (35), but their regulation remains largely unknown. On the contrary, the activity of the ATP synthase is regulated at various levels, one being the redox state of the thioredoxin system, which senses the redox state of the stroma/cytosol. Oxidizing conditions result in the inactivation of the ATP synthase (36, 37). The ATP synthase is also regulated by the trans-membrane potential itself: when it stands below a "critical" threshold the ATP synthase is partially inactivated (38). In green algae, diatoms and plants, this has been used to demonstrate that a permanent trans-thylakoid electrochemical potential is maintained in the dark by the reversed activity of the ATP synthase, which hydrolyses the ATP produced in the mitochondria and imported in the chloroplast (16, 17, 39). When inhibiting mitochondrial respiration, the trans-thylakoid electrochemical proton gradient decreases in darkness and the ATP synthase switches to a

partially inactive form. Because of the lower value of the electrochemical proton gradient in the dark, its subsequent increase during a saturating pulse of light is larger (16). In cyanobacteria, the thylakoid membranes house both the respiratory and the photosynthetic chains. Therefore, one can expect that a high trans-thylakoid electrochemical gradient of protons is maintained in the dark by the ongoing respiration. Respiration can be suppressed by a prolonged (24h or more) incubation in complete darkness, resulting in the depletion of respiratory substrates (5). The prolonged dark incubation also causes the oxidation of the electron transport chain and, presumably, of the cytosol. We tested the effects of dark starvation on the membrane potential decay in *S. elongatus* (representative traces in Fig. 4, average of 3 biological replicates in Fig S10A and B). In light-grown cells briefly dark-adapted, the flash-induced increase in electric field was dissipated in about 50 ms (Fig 4B), a time shorter than that observed in green algae (13), suggesting a higher ATP synthase/counter-ion exchange activity and, therefore, a high transmembrane electric field pre-existing in darkness and reducing conditions. Dark starved cells showed a marked decrease in the decay rate of the ECS signal. The flash-induced decay kinetics increased again when dark starved cells were re-incubated in the light for 2 hours (recovery). The effect of dark starvation was thus reversible when a pool of respiratory substrates (and therefore of reductants) was re-generated by photosynthetic activity. We note that starvation in darkness also increased the amplitude of the electric field generated during a pulse of saturating light (Fig. 4C), while concomitantly slowing down its decay. This demonstrates that the transmembrane electric field in darkness had collapsed upon starvation and oxidizing conditions were established. Again, recovery in the light increased the ECS decay rate. We verified that dark starvation also modified the decay kinetics of *Synechocystis* (Fig. S10D). Addition of the ATP synthase inhibitor venturicidin to dark starved cells further slowed down the ECS decay, whereas the subsequent addition of the uncoupler CCCP re-accelerated it (Fig. 4D). This indicates that dark starvation of *S. elongatus* leads to a partial down-regulation of the ATP synthase activity but not to its complete inactivation. In dark-starved cells of *S. elongatus* treated with venturicidin, the ECS increase generated by applying 100 µs light pulses given at short time intervals could be integrated in a linear manner, owing to its very slow decay (Fig. S10C), further demonstrating that the ECS (measured as the difference between 500-505 and 480-485 nm absorption changes) depends linearly upon the electric field. It is of note that the integration properties and the opposite effects of ATP synthase inhibitors and ionophores on the decay phase further confirmed that we measure a *bona fide* ECS signal which probes the actual electric field across the thylakoid membranes. Clearly, we

cannot exclude that membrane permeability changes induced by dark starvation also depend on changes in counter-ion exchanges. Since it provides a direct measurement of the trans-thylakoid potential, ECS is ideally suited to study further the *in vivo* activity of ion channels in thylakoid membranes of cyanobacteria.

ECS-based measurements of steady-state electron flows in S. elongatus and Synechocystis

In chloroplasts, Cyclic Electron Flow (CEF) around PSI is considered a major way to generate a proton motive force without the net production of NADPH and, therefore, to ensure the correct ATP:NADPH ratio for carbon assimilation, which cannot be provided by the sole Linear Electron Flow (LEF) (40, 41). This constraint may be different in cyanobacteria, where the interconnection of the photosynthetic and respiratory electron transport pathways and other alternative electron fluxes (3, 42) could balance the production ratio of ATP and NADPH. Here, instead of using the concepts of "linear" and "cyclic" electron flows, we rather distinguished between "total" and "PSII-independent" electron flows. We investigated the steady-state Total Electron Flow (TEF - when both photosystems are active) and the PSII-independent Electron Flow (PSII-independent EF - in presence of DCMU and HA) rates in *S. elongatus* and *Synechocystis*. We used the ECS signals to perform Dark Interval Relaxation Kinetics ($DIRK_{(ECS)}$) measurements (15), as detailed in the Supplementary Materials and Methods. Stationary photochemical rates were established by adapting the cells for several minutes to increasing intensities of constant actinic light. Fig. 5A and B show the dependency on the actinic light intensity of the electron flows measured in the two cyanobacteria. In both cases, the TEF rates showed a dependency on light intensity that saturated at 20 to 35 e/s/PSI (light intensity of approximately 350 µmol photons/m^2/s), depending on the experiment. On the contrary, the PSII-independent EF did not exceed 2-7 e/s/PSI at any light intensity. Accordingly, the PSII and PSI yields measured in the same conditions as the $DIRK_{(ECS)}$ also showed a strong dependency on light intensity in absence of inhibitors, with the PSI yields collapsing in presence of DCMU and HA, which is consistent with the low PSII-independent EF (Fig. S11). It is of note that these slow PSI turnover rates in absence of PSII electron donation were not due to a strong derivation of reductants towards highly active cyanobacterial respiratory oxidases, since their inhibition with KCN did not cause an increase in the PSII-independent EF rates measured (Fig. S12). This low electron flow, similar to what is observed in the same experimental conditions in eukaryotic photosynthesis (43), does not qualify cyanobacterial NDH - despite its high affinity for reduced ferredoxin presumably

produced by PSI (44) - as a PSII by-passing enzyme specifically dedicated to cyclic electron flow in prokaryotic photosynthesis.

Our observation is consistent with a previous report of low PSI turnover rates measured in cyanobacteria in presence of DCMU through P_{700}^{+} absorption spectroscopy (45). We note however that much higher rates, attributed to CEF, have been reported in chloroplasts in transient situations (14) and more sustained "PSI-only" electron flow may occur when PSII is active. In addition, in *S. elongatus*, DCMU was reported to prevent an even distribution of the NDH-1 complex in the thylakoid membranes upon moderate illumination, maintaining it aggregated in distinct spots as in the dark (46). Thus, one should also consider that a spatial segregation of NDH complexes may contribute to the low level of PSII-independent EF that we measured.

Conclusions

We have shown that ECS signals, likely corresponding to carotenoid band shifts originating from the PSI cores, are present in both *S. elongatus* and *Synechocystis*. These ECS signals respond linearly to the electric field and can be best measured in these cyanobacteria in the 480-505 nm region. Even though the absorption changes in this region include other contributions, the difference between absorption changes at 500-505 nm and 480-485 nm provide measures of ECS cleared from those contributions. The ECS signals measured this way display classical flash-induced kinetics: a fast rise reflecting photosystem activity (sensitive to inhibitors of PSII), a slower rise dependent on cytochrome b_6f activity (sensitive to PMS and DBMIB), and a decay phase reflecting the electric permeability of the membrane (sensitive to uncouplers and ATPase inhibitors).

Although an extensive investigation of the physiology of the various electron transport pathways is beyond the scope of the present study, we showed here that a direct measure of the electric field resulting from the photosynthetic activity can provide unique information to understand cyanobacterial bioenergetics. Through the development of oxygenic photosynthesis, cyanobacteria greatly influenced the evolution of life on Earth and are organisms of high ecological and biotechnological relevance. For these reasons, the development of ECS-based physiological measurements should be instrumental in a better understanding the complex metabolism of these organisms.

Materials and Methods

Cyanobacteria cultures - *Synechococcus elongatus* PCC7942 and *Synechocystis sp.* PCC6803 (respectively *S. elongatus* and *Synechocystis* in the following) strains were kindly provided by Diana Kirilovsky. The *Synechocystis* PAL mutant was kindly provided by Ghada Ajlani; the *Synechocystis* PSII- mutant was generated and characterized as described in the SI Appendix. Cells were grown under white light (30-35 µmol photons/m^2/s) in BG11 medium (supplemented with 5 mM glucose in the case of the PAL and PSII- mutants) with constant shaking.

Inhibitors - 3-(3,4-dichlorophenyl)-1,1-dimethylurea (DCMU), 2,5-dibromo-3-methyl-6-isopropylbenzoquinone (DBMIB) and carbonyl cyanide m-chlorophenyl hydrazone (CCCP) were dissolved in ethanol; hydroxylamine (HA), 5-Methylphenazinium methyl sulphate (PMS), venturicidin and potassium cyanide (KCN) were dissolved in water. Final concentrations used: 20 µM DCMU, 500 µM HA, 40 µM venturicidin, 100 µM CCCP, 15 µM PMS, 40 µM DBMIB,50 µM KCN.

Spectroscopy measurements – Two experimental setups were used in this work. Full details on the light sources and filters used are given in the SI Appendix.

A home-made Optical Parametric Oscillator (OPO)-based spectrophotometer (47) having a time resolution of 10 ns was used for fast (<50 µs) measurements and for spectra recording in the 410 - 570 nm region. Cells were injected in two closed horizontal cuvettes, one used on the reference and one on the measuring photodiodes. In this setup, the measuring beam is split between the two cuves, whereas the actinic light illuminates only one of the two. The absorption changes induced by the measuring light alone are automatically subtracted from those measured with actinic illumination, to correct for actinic effects of the measuring light. The cells were incubated in the cuves in presence of specified inhibitors in the dark for 30 minutes before the experiments, in anaerobic conditions. The spectra were recorded back and forth from 570 nm to 410 nm and the back and forth recordings were averaged to correct for sedimentation or physiological changes occurring during the experiment. A total of 8 actinic flashes were integrated for each wavelength. For the measurement of open PSI (Fige 3) at time *t* after a saturating flash, the fraction of reduced P_{700} was measured as the difference between the $\Delta I/I$435 nm at time *t* and the one at 5 ms, normalized by the difference between

the $\Delta I/I$ 435 nm at 200 ns (fully oxidized PSI) and the one at 5 ms. In parallel, we measured the ECS increase ($\Delta I/I$ 500-485 nm) 5 ms after two single turnover flashes separated by a time interval *t*. The difference between the ECS increase after 2 flashes and the one after a single flash is equal to the contribution to ECS of PSI centres which reopened between the 2 flashes. This value was normalized by the maximal value obtained when the two actinic flashes were separated by 5 ms.

A LED-based spectrophotometer (JTS10, Biologic, France) was used for measurements of fluorescence and absorbance kinetics. In this setup, in the case of absorption changes, all measurements were performed in presence and absence (measuring light only) of actinic illumination on each biological sample. The absorption changes induced by the measuring light alone (actinic effects or changes in the LED output intensity due to heating) were then subtracted from those recorded in presence of actinic illumination. Representative traces are shown in Fig. S1. For single-turnover flash and saturating light pulse measurements cells were injected in a closed horizontal cuvette in presence of the specified inhibitors and manually re-oxygenated every few minutes. For longer measurements in continuous light, cell samples were deposited in the cavity of a horizontal cuvette overlaid with a semi-permeable membrane separating them from a second cavity were a constant flow of air was pumped. PSII and PSI photosynthetic yields were calculated as in (7) and (8), respectively. Photochemical rates measurements were performed using Dark Interval Relaxation Kinetics ($DIRK_{(ECS)}$) as described in the SI Appendix.

Acknowledgements. This work was supported by UMR7141, CNRS/Sorbonne Université and by the Agence Nationale de la Recherche (ReCyFuel: ANR-16-CE05-0026-01). B. Bailleul also acknowledges the support by the European Research Council (ERC) PhotoPHYTOMIX project (grant agreement No. 715579). We thank Diana Kirilovsky and Pierre Sétif for the fruitful discussions and Stefano Santabarbara for his critical reading of the manuscript. We thank Jianfeng Yu and Peter Nixon for kindly sharing the *Synechocystis* PSII-mutant and Ghada Ajlani for the *Synechocystis* PAL mutant.

References

1. Dismukes GC, et al. (2001) The origin of atmospheric oxygen on Earth: The innovation of oxygenic photosynthesis. *Proc Natl Acad Sci* 98(5):2170–2175.

2. Nowicka B, Kruk J (2016) Powered by light: Phototrophy and photosynthesis in prokaryotes and its evolution. *Microbiol Res* 186–187:99–118.

3. Mullineaux CW (2014) Co-existence of photosynthetic and respiratory activities in cyanobacterial thylakoid membranes. *Biochim Biophys Acta - Bioenerg* 1837(4):503–511.

4. Mi H, Endo T, Schreiber U, Asada K (1992) Donation of electrons from cytosolic components to the intersystem chain in the cyanobacterium *Synechococcus sp.* PCC 7002 as determined by the reduction of P700+. *Plant Cell Physiol* 33(8):1099–1105.

5. Mi H, Endo T, Schreiber U, Ogawa T, Asada K (1994) NAD(P)H dehydrogenase-dependent cyclic electron flow around Photosystem-I in the cyanobacterium *Synechocystis* PCC6803 - A study of dark-starved cells and spheroplasts. *Plant Cell Physiol* 35(2):163–173.

6. Yeremenko N, et al. (2005) Open reading frame *ssr2016* is required for antimycin A-sensitive photosystem I-driven cyclic electron flow in the cyanobacterium *Synechocystis sp*. PCC 6803. *Plant Cell Physiol* 46(8):1433–1436.

7. Genty B, Briantais JM, Baker NR (1989) The relationship between the quantum yield of photosynthetic electron transport and quenching of chlorophyll fluorescence. *Biochim Biophys Acta - Gen Subj* 990(1):87–92.

8. Klughammer C, Schreiber U (1994) An improved method, using saturating light pulses, for the determination of photosystem I quantum yield via P700+-absorbance changes at 830 nm. *Planta* 192(2):261–268.

9. Ogawa T, Misumi M, Sonoike K (2017) Estimation of photosynthesis in cyanobacteria by pulse-amplitude modulation chlorophyll fluorescence: problems and solutions. *Photosynth Res* 133(1–3):63–73.

10. Remelli W, Santabarbara S (2018) Excitation and emission wavelength dependence of fluorescence spectra in whole cells of the cyanobacterium *Synechocystis sp.* PPC6803:

Influence on the estimation of Photosystem II maximal quantum efficiency. *Biochim Biophys Acta - Bioenerg* 1859(11):1207–1222.

11. Witt HT (1979) Energy converstion in the functional membrane of photosynthesis. analysis by light pulse and electric pulse methods. *Biochim Biophys Acta* 505:355–427.

12. Bailleul B, Cardol P, Breyton C, Finazzi G (2010) Electrochromism: A useful probe to study algal photosynthesis. *Photosynth Res* 106(1–2):179–189.

13. Joliot P, Delosme R (1974) Flash-induced 519 nm absorption change in green algae. *BBA - Bioenerg* 357(2):267–284.

14. Joliot P, Joliot A (2002) Cyclic electron transfer in plant leaf. *Proc Natl Acad Sci* 99(15):10209–10214.

15. Sacksteder CA, Kanazawa A, Jacoby ME, Kramer DM (2000) The proton to electron stoichiometry of steady-state photosynthesis in living plants: A proton-pumping Q cycle is continuously engaged. *Proc Natl Acad Sci* 97(26):14283–14288.

16. Joliot P, Joliot A (2008) Quantification of the electrochemical proton gradient and activation of ATP synthase in leaves. *Biochim Biophys Acta - Bioenerg* 1777(7–8):676–683.

17. Bailleul B, et al. (2015) Energetic coupling between plastids and mitochondria drives CO_2 assimilation in diatoms. *Nature* 524(7565):366–369.

18. Schmidt S, Reich R, Witt HT (1971) Electrochromism of chlorophylls and carotenoids in multilayers and in chloroplasts. *Naturwissenschaften* 58(8):414.

19. Fork DC, Amesz J (1967) Light-induced shifts in the absorption spectrum of carotenoids in red and brown algae. *Photochem Photobiol* 6(12):913–918.

20. Amesz J, Visser JWM (1971) Light-induced shifts in pigment absorption in green, red and blue-green algae. *BBA - Bioenerg* 234(1):62–69.

21. Holmes NG, Hunter CN, Niederman RA, Crofts AR (1980) Identification of the pigment pool responsible for the flash-induced carotenoid band shift in *Rhodopseudomonas sphaeroides* chromatophores. *FEBS Lett* 115(1):43–48.

22. Hirano M, Katoh S (1981) Electrochromic band shifts of carotenoid in a blue-green

alga. *Photochem Photobiol* 34(5):637–643.

23. Bailleul B, et al. (2008) The thermodynamics and kinetics of electron transfer between cytochrome b_6f and photosystem I in the chlorophyll d-dominated cyanobacterium, *Acaryochloris marina*. *J Biol Chem* 283(37):25218–25226.

24. Frese RN, et al. (2002) Electric field effects on red chlorophylls, beta-carotenes and P700 in cyanobacterial Photosystem I complexes. *Biochim Biophys Acta - Bioenerg* 1554(3):180–191.

25. Alric J, Pierre Y, Picot D, Lavergne J, Rappaport F (2005) Spectral and redox characterization of the heme ci of the cytochrome b_6f complex. *Proc Natl Acad Sci* 102(44):15860–15865.

26. Forti G, Rosa L (1971) On the pathway of electron transport in cyclic photophosphorylation. *FEBS Lett* 18(1):55–58.

27. Racker E, Hauska GA, Lien S, Berzborn RJ, Nelson N (1972) Resolution and reconstitution of the system of photophosphorylation. *Photosynthesis, Two Centuries after Its Discovery by Joseph Priestley*, pp 1097–1113.

28. Ajlani G, Vernotte C (1998) Construction and characterization of a phycobiliprotein-less mutant of *Synechocystis sp.* PCC 6803. *Plant Mol Biol* 37(3):577–580.

29. Liberton M, et al. (2017) Phycobilisome truncation causes widespread proteome changes in *Synechocystis sp.* PCC 6803. *PLoS One* 12(3):1–18.

30. Witt H, et al. (2003) Species-specific differences of the spectroscopic properties of P700: Analysis of the influence of non-conserved amino acid residues by site-directed mutagenesis of photosystem I from *Chlamydomonas reinhardtii*. *J Biol Chem* 278(47):46760–46771.

31. Haehnel W, Hesse V, Pröpper A (1980) Electron transfer from plastocyanin to P700. Function of a subunit of photosystem I reaction center. *FEBS Lett* 111(1):79–82.

32. Delosme R, Zickler A, Joliot P (1978) Turnover kinetics of Photosystem I measured by the electrochromic effect in Chlorella. *BBA - Bioenerg* 504(1):165–174.

33. Farah J, Rappaport F, Choquet Y, Joliot P, Rochaix JD (1995) Isolation of a psaF-

deficient mutant of *Chlamydomonas reinhardtii*: efficient interaction of plastocyanin with the photosystem I reaction center is mediated by the PsaF subunit. *EMBO J* 14(20):4976–4984.

34. Fraser JM, et al. (2013) Photophysiological and photosynthetic complex changes during iron starvation in *Synechocystis sp.* PCC 6803 and *Synechococcus elongatus* PCC 7942. *PLoS One* 8(3). doi:10.1371/journal.pone.0059861.

35. Checchetto V, et al. (2012) Thylakoid potassium channel is required for efficient photosynthesis in cyanobacteria. *Proc Natl Acad Sci* 109(27):11043–11048.

36. Ort DR, Oxborough K (2003) In Situ Regulation of Chloroplast Coupling Factor Activity. *Annu Rev Plant Physiol Plant Mol Biol* 43(1):269–291.

37. Hisabori T, Sunamura E-I, Kim Y, Konno H (2012) The chloroplast ATP synthase features the characteristic redox regulation machinery. *Antioxid Redox Signal* 19(15):1846–1854.

38. Junge W (1970) The critical electric potential difference for photophosphorylation: Its relation to the chemiosmotic hypothesis and to the triggering requirements of the ATPase system. *Eur J Biochem* 14(3):582–592.

39. Diner B, Joliot P (1976) Effect of the transmembrane electric field on the photochemical and quenching properties of Photosystem II in vivo. *BBA - Bioenerg* 423(3):479–498.

40. Bendall DS, Manasse RS (1995) Cyclic photophosphorylation and electron transport. *BBA - Bioenerg* 1229(1):23–38.

41. Shikanai T (2007) Cyclic electron transport around Photosystem I: genetic approaches. *Annu Rev Plant Biol* 58(1):199–217.

42. Lea-Smith DJ, Bombelli P, Vasudevan R, Howe CJ (2016) Photosynthetic, respiratory and extracellular electron transport pathways in cyanobacteria. *Biochim Biophys Acta - Bioenerg* 1857(3):247–255.

43. Alric J (2010) Cyclic electron flow around photosystem I in unicellular green algae. *Photosynth Res* 106(1–2):47–56.

44. Schuller JM, et al. (2018) Structural adaptations of photosynthetic complex I enable ferredoxin-dependent electron transfer. *Science* 363(6424):257–260.

45. Myers J (1987) Is there significant cyclic electron flow around photoreaction 1 in cyanobacteria? *Photosynth Res* 14(1):55–69.

46. Liu LN, et al. (2012) Control of electron transport routes through redox-regulated redistribution of respiratory complexes. *Proc Natl Acad Sci* 109(28):11431–11436.

47. Joliot P, Béal D, Rappaport F (1998) A new high-sensitivity 10-ns time-resolution spectrophotometric technique adapted to *in vivo* analysis of the photosynthetic apparatus, In: Photosynthesis: Mechanisms and Effects, Garab G. eds. (Springer, Dordrecht), pp 4247–4252.

Figure Legends

Fig. 1. Absorption difference signals in *S. elongatus* and *Synechocystis*. (A) Spectra of flash-induced absorption changes in *S. elongatus* cells treated with DCMU and HA. (B, C) Spectra of flash-induced absorption changes in *S. elongatus* and *Synechocystis* cells, respectively, determined in presence of DCMU and HA and 15 µM PMS. Absorption changes were sampled at the indicated time intervals after the flash (in ms). Note that for all the spectra the y axis of the 410-450 nm region has a different scale.

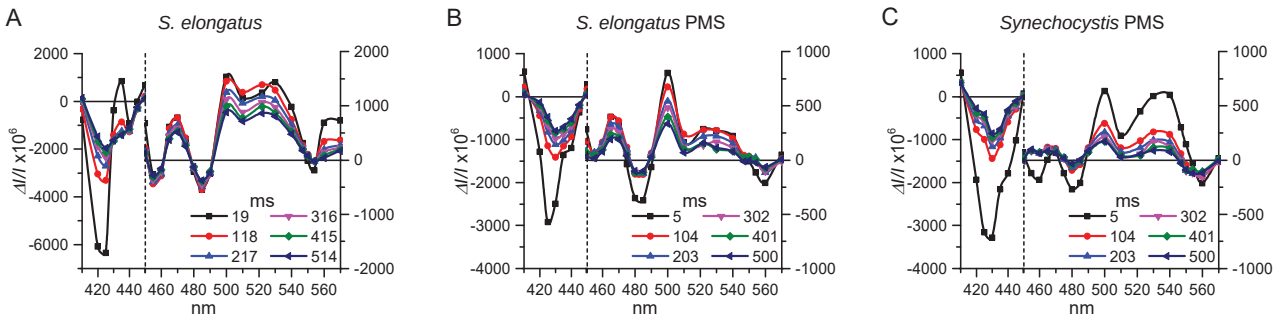
Fig. 2. Spectra of flash-induced absorption changes in *Synechocystis* wild type (WT) and mutants determined in presence of DCMU, HA and PMS. The spectra are normalized on the 500 – 485 nm difference. The inserts represent the 450-530 nm region on an expanded scale. (A) Comparison between wild type and PSII- mutant spectra taken at 100 ms after the flash. (B) Comparison between wild type and PAL mutant at 5 ms after a flash.

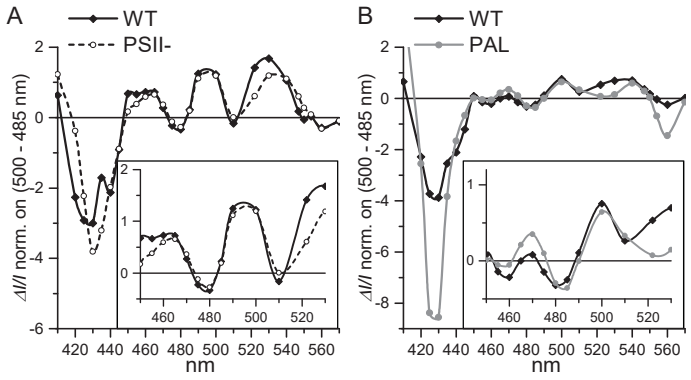
Fig. 3. Comparison of ECS and P_{700}^{+} methods to measure PSI photochemistry in *S. elongatus* and *Synechocystis*. Experiments were performed in presence of DCMU, HA and PMS. (A) and (B) ECS signals (500 - 485 nm) in *S. elongatus* and *Synechocystis*, respectively, measured after a single flash and after two flashes fired at 5 ms time interval and normalized to those generated by the single flash, corresponding to 1 charge separation/PSI (3 biological replicates ± s.d.). The value of the second flash with respect to the single one was 1.89±0.07 for *S. elongatus* and 1,93±0.04 for *Synechocystis*. (C) Fraction of PSI open centres as a function of the time after the first flash, measured as the ECS increase upon a second flash (see Methods). (D) Comparison between PSI open centres measured with ECS (panel C) or with through the kinetics of reduction of P_{700}^{+}, measured as the absorption difference at 435 nm. The dashed lines represent the linear fit of the experimental points.

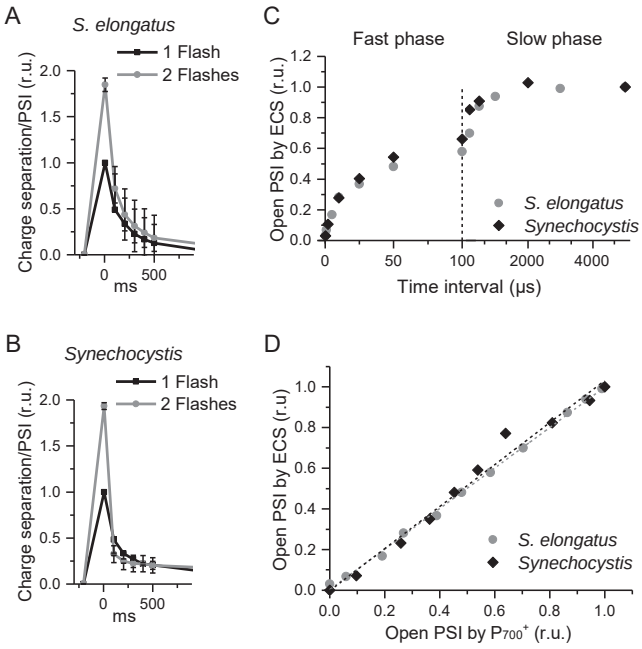
Fig. 4. ECS kinetics in light-grown and dark-starved *S. elongatus* cells. (A) Representative kinetics of flash-induced ECS signals (503 - 480 nm) in *S. elongatus* cells without (Control) and with the addition of PSII inhibitors (DCMU and HA). (B) Representative kinetics of flash-induced ECS signals measured in light-grown cells (Light), after 24 h of dark starvation (Dark) and in dark-starved cells after 2 h of recovery in the light (Dark+Rec). (C) Membrane potential kinetics measured with ECS (normalized on the single-turnover flash) during saturating light pulses in the same samples as in (B). The pulse duration was adjusted to reach the maximal potential levels, the time-point 0 is at the pulse offset. (D) Membrane potential kinetics measured with ECS (normalized on the single-turnover flash) during saturating light

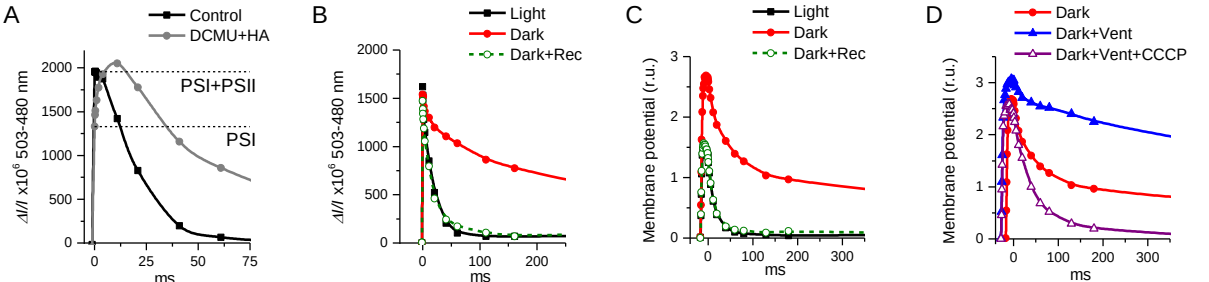
pulses in dark starved cells (same as panel C) and in dark starved cells in presence of venturicidin without or with the further addition of the uncoupler CCCP.

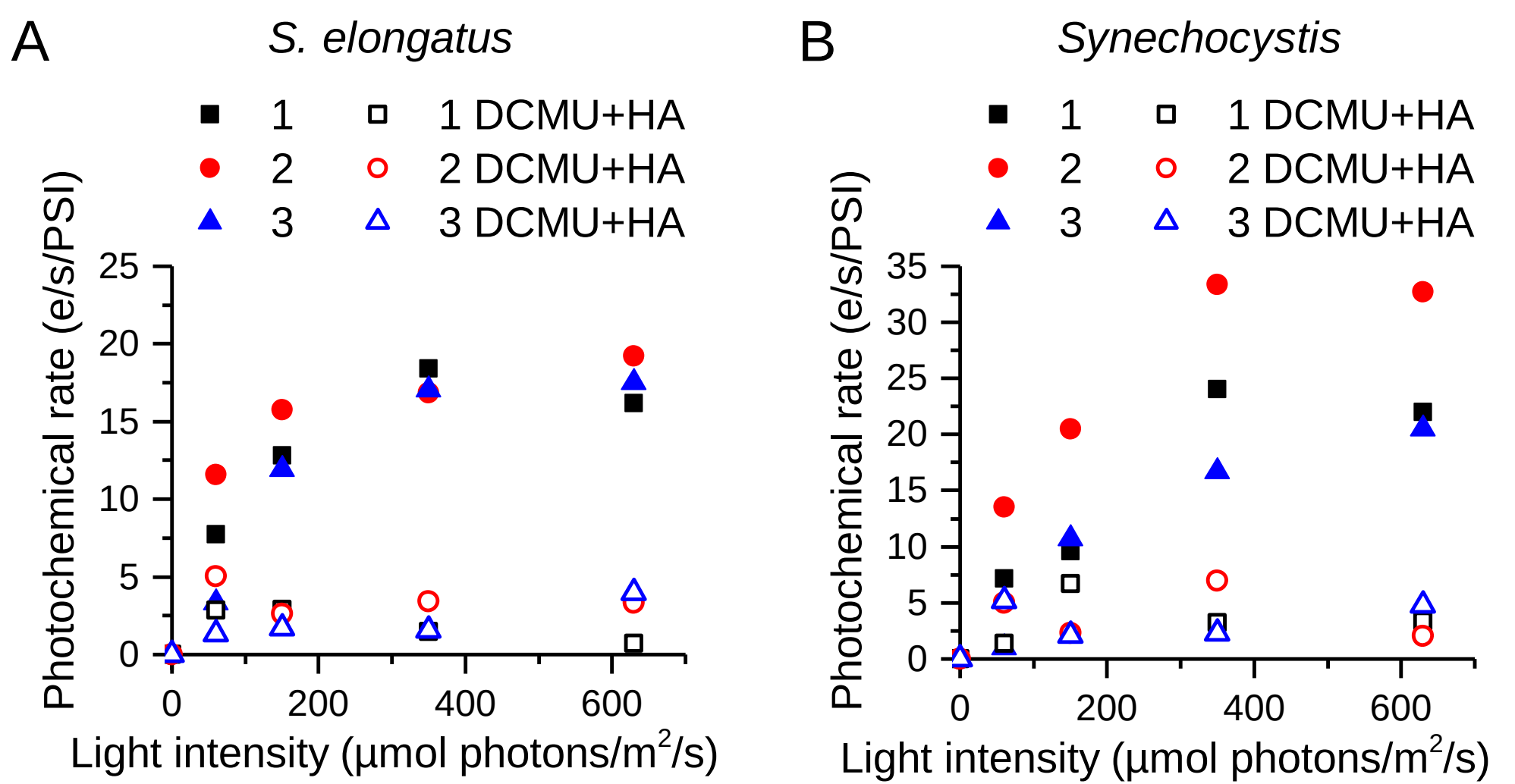
Fig. 5. Total (solid symbols) and PSII-independent (in presence of DCMU and HA, open symbols) electron flow capacities in *S. elongatus* (A) and *Synechocystis* (B) cells. Electron flows were measured at increasing intensities of constant light using the $DIRK_{(ECS)}$ method. Rates are normalized on the single-turnover flash in presence of DCMU and HA (i.e. per PSI) and correspond to 3 independent biological replicates.


A
S. elongatus
B
S. elongatus PMS
C
Synechocystis PMS
ΔI/I x10^6
nm
ms
19
118
217
316
415
514
5
104
203
302
401
500


A
WT
PSII-
B
WT
PAL
ΔI/I norm. on (500 - 485 nm)
nm


A
S. elongatus
1 Flash
2 Flashes
Charge separation/PSI (r.u.)
2.0
1.5
1.0
0.5
0.0
0
500
ms
B
Synechocystis
1 Flash
2 Flashes
Charge separation/PSI (r.u.)
2.0
1.5
1.0
0.5
0.0
0
500
ms
C
Fast phase
Slow phase
Open PSI by ECS (r.u.)
1.2
1.0
0.8
0.6
0.4
0.2
0.0
0
50
100
2000
4000
Time interval (µs)
S. elongatus
Synechocystis
D
Open PSI by ECS (r.u)
1.0
0.8
0.6
0.4
0.2
0.0
0.0
0.2
0.4
0.6
0.8
1.0
Open PSI by P700+ (r.u.)
S. elongatus
Synechocystis


A
Control
DCMU+HA
PSI+PSII
PSI
ΔI/I x10^6 503-480 nm
ms
B
Light
Dark
Dark+Rec
ΔI/I x10^6 503-480 nm
ms
C
Light
Dark
Dark+Rec
Membrane potential (r.u.)
ms
D
Dark
Dark+Vent
Dark+Vent+CCCP
Membrane potential (r.u.)
ms


A
S. elongatus
1
1 DCMU+HA
2
2 DCMU+HA
3
3 DCMU+HA
Photochemical rate (e/s/PSI)
0
5
10
15
20
25
0
200
400
600
Light intensity (µmol photons/m2/s)
B
Synechocystis
1
1 DCMU+HA
2
2 DCMU+HA
3
3 DCMU+HA
Photochemical rate (e/s/PSI)
0
5
10
15
20
25
30
35
0
200
400
600
Light intensity (µmol photons/m2/s)